H. R. Imani JAJARMI, Azah MOHAMED, H. SHAREEF, SUBIYANTO

Department of Electrical, Electronic, and Systems Engineering, Universiti Kebangsaan Malaysia

Adaptive interval type2 fuzzy hysteresis-band current-controlled active power filter for power quality improvement

Abstract. *This paper presents a novel adaptive hysteresis current control based on interval type2 fuzzy logic for active power filter to eliminate harmonics and compensate for reactive power. A new method to generate reference compensating current for the fundamental active current component is also proposed using the recursive discrete Fourier transform. The switching frequency of the conventional fixed hysteresis band (HB) control during the fundamental period is varied; thus causing harmonic ripple of the load current. This problem can be solved using adaptive HB control strategy. In this study, a fuzzy logic controller is used for base control because of its advantages over other adaptive HB techniques, such as mathematical simplicity, ease in adding heuristic knowledge, and robust changes in system operating conditions. An interval type2 fuzzy-adaptive HB technique is utilized for the current control to enhance the switching signals produced by the voltage source inverter. Based on the supply voltage and the slope of the reference current, this controller changes the hysteresis bandwidth. To control the DC capacitor voltage, an interval type2 fuzzy logic based controller is developed. Simulation results of the shunt active power filter with an interval type2 fuzzy adaptive HB current controller are examined and compared with the conventional controller. The results verify the effectiveness of the proposed controller in reducing total harmonic distortion from 21.03% to 2.12% and reactive power from 2616 Var to 6.28Var.*

Streszczenie. *Zapresentowano nową metodę adaptacyjnego sterowanie prądem w celu eliminacji harmonicznych i kompensacji mocy biernej. Wykorzystano aktywny filtr bazujący na logice rozmytej typu 2. Stosuje się adaptacyjne histerezowe sterowanie w celu poprawy sygnału przełączania wytwarzanego przez przekształtnik napięciowy. Sterownik zmienia szerokość histerezy bazując na wartości napięcia zasilaniam i szybkości zmian pradu. Zmniejszono zawartość harm onicznych z 21% do 2 % i moc bierna z 2616 Var do 6,3 VAR.* ***Adaptacyjny filtr aktywny do poprawy jakości mocy bazujący na sterownku histerezowym fuzzy logic***

Keywords: Active power filter, Recursive discrete Fourier transform, Interval type-2 fuzzy, Power quality conditioning.
Słowa kluczowe: kompensacja mocy biernej, filtr aktywny, logika rozmyta.

doi:10.12915/pe.2014.09.37

Introduction

The main cause of harmonic current generation is the use of nonlinear loads such as electronic power supplies, rectifiers, and static power converters [1]. Most nonlinear loads contribute to poor power factors, reactive power burdens, unbalanced power, and other problems that lead to lower system efficiency, thus creating serious power-quality problems. Harmonic distortion and the effects of power quality on the power system increased because of industrial development and heavy use of power electronics. The use of active power filter (APF) is widely accepted and is considered an effective method to compensate current and voltage distortions. [2–3]. To mitigate harmonics in a power system, APF generates suitable compensating current/voltage signals that cancel the harmonic components of the load by a control algorithm. Hence, proper selection of control algorithm is an important factor influencing the APF performance. Commonly, the control algorithm measures certain parameters such as load currents, DC bus voltage, and source voltage to calculate the compensating currents of the APF [4]. Harmonic currents/voltages are detected by measuring these signals; thus, the amount of compensating currents/voltages in the opposite direction of the harmonic current/voltage that is required for feeding back into the power system are calculated [5].

Techniques for current/voltage reference estimation are classified as time–domain control and frequency–domain control techniques. Among the most widely used frequency–domain techniques are the conventional Fourier, fast Fourier transform algorithm [6], modified Fourier series techniques [7], discrete Fourier Transform (DFT) [8], and recursive discrete Fourier transform (RDFT) [9]. Time–domain techniques include the differential quadrature method [6], instantaneous reactive power algorithm [10], synchronous detection method [11], and synchronous reference frame theory [12]. In this study, an approach using an RDFT filter block (Fig. 3) to generate reference currents is presented. The fundamental load current component is determined using the block and is then multiplied by $\sin \omega t$. A desired DC component $I_p/2$ and the rest of the AC components are determined using the characteristics of the triangle function. It is multiplied by two to obtain the peak value of the fundamental active current ($I_p = I_1 \cos \Phi_1$). The resulting value is added to the output of the DC capacitor voltage regulator, which is produced by the interval type2 fuzzy logic controller (IT2FLC). The peak source currents are then produced. The product of the signal and the unit vectors of the three-phased source voltage will generate the desired source side current. The reference currents of APFs can finally be obtained by subtracting the desired source side currents from the load currents. Various pulse-width modulation (PWM) techniques are used to generate the switching patterns of the triggering signals of the insulated-gate bipolar transistors (IGBTs) that determine the required compensation for current harmonics. The hysteresis-band (HB) current control method with a fixed HB is one of the most commonly used modulation techniques for voltage-fed PWM converters. Despite several advantages such as easy implementation, fast-response current loop, lack of tracking error, and good dynamics, this method operates at variable switching frequency, which increases switching losses and excessive ripples in the source current. An adaptive HB current control technique as an active filtering function can be implemented to minimize the effect of current distortions on modulated waveforms [13]. IT2FLC is used in this study because of its applicability for uncertainty and imprecision and is considered more efficient than the type-1 fuzzy logic controller. Studies showed that the IT2FLC performs more efficiently compared with the type-1 fuzzy logic controller [14].

Shunt Active Power Filter

A. Reference source current

To enhance the APF performance, the reference source current should be correctly generated. The control strategy for a SAPF generates the reference current. The power filter compensates the reactive power and harmonic currents by providing current references. Fig.1 shows the block diagram of the implemented fuzzy logic control scheme of a shunt active power filter.

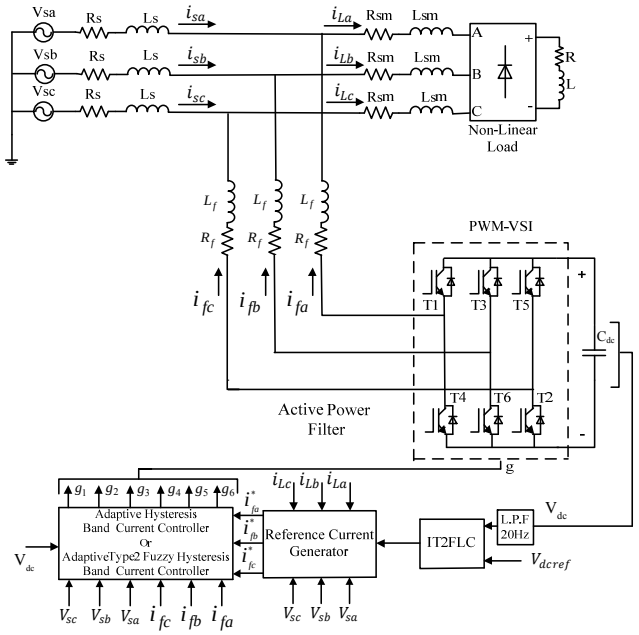

Fig. 1. Closed-loop Fuzzy Logic-Controlled SAPF

B. Estimation of Compensation Current Reference

Ideal compensation occurs when the mains current is sinusoidal and in phase with the source voltage, regardless of the nature of the load. After compensation, the desired source currents can be presented in the following form [15]:

(1) $$i_{sa}^{*} = I_{sp}\sin\omega t,\ i_{sb}^{*} = I_{sp}\sin(\omega t - 120^{O}),$$
$$i_{sc}^{*} = I_{sp}\sin(\omega t + 120^{O})$$

where I_{sp} and ω are the amplitudes of the desired source current and angular frequency, respectively. The phase angle can be obtained from the source. The phase of the source currents are known, whereas the source current magnitudes have to be determined. Assuming that the power supply voltage is a sine wave (phase A),

(2) $$V_{sa}(t) = V_m \sin\omega t$$

By Fourier transformation, the load current $i_{La}(t)$ can be decomposed as follows:

(3) $$i_{La}(t) = \sum_{n=1}^{\infty} I_n \sin(n\omega t + \Phi_n) = I_1 \sin(\omega t + \Phi_1) + \sum_{n=2}^{\infty} I_n \sin(n\omega t + \Phi_n) = I_1 \sin\omega t \cos\Phi_1 + I_1 \cos\omega t \sin\Phi_1 + \sum_{n=2}^{\infty} I_n \sin(n\omega t + \Phi_n) = i_1(t) + i_h(t) = i_{1p}(t) + i_{1q}(t) + i_h(t)$$

where I_n, Φ_n represent the peak value and the phase angle of the n-order harmonic current, respectively; n is a positive integer; I_1, Φ_1 denote the peak value and the phase angle of the fundamental load current, respectively. $I_{1p}(t)$ represents the fundamental active current component, $I_{1q}(t)$ is the fundamental reactive current component, and $i_h(t)$ is the harmonic current component. From Equation (3), the following equations are deduced:

(4) $$i_{1p}(t) = I_p \sin\omega t$$

(5) $$i_{1q}(t) = I_q \cos\omega t$$

(6) $$i_h(t) = \sum_{n=2}^{\infty} I_n \sin(n\omega t + \Phi_n)$$

where $I_p = I_1\cos\Phi_1, I_q = I_1\sin\Phi_1$ and I_p, I_q are the peak values of the fundamental active current and reactive current, respectively. Thus, the value of I_p can be determined from the value of I_{1p}. Multiplying the fundamental current $i_1(t)$ (determined by an RDFT filter block) by $\sin\omega t$ results in the following triangle function characteristic:

(7) $$i_1(t)\sin\omega t = I_p \sin^2\omega t + I_q \cos\omega t.\sin\omega t = \frac{I_p}{2}(1-\cos 2\omega t) + \frac{I_q}{2}\sin 2\omega t$$

The triangle function characteristic comprises the DC component $(\frac{I_p}{2})$ and the AC component $(-\frac{I_p}{2}\cos 2\omega t + \frac{I_q}{2}\sin 2\omega t)$. To separate the DC and AC components in the simulation of this module, the mean value block is implemented because the average value of a sine wave over a full cycle is zero. Therefore, the DC component $\frac{I_p}{2}$ can also be determined by calculating the average value. I_p can be obtained (the first component of the amplitude of the desired source current) after multiplying the DC component by two. The second component of the AC source current (I_{sl}) is obtained from the DC capacitor voltage regulator, as shown in Fig. 2.

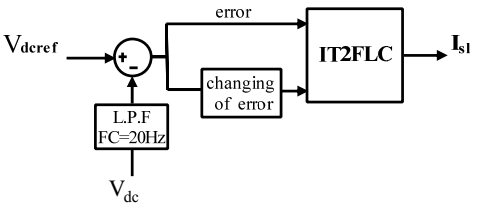

Fig. 2. Structure of AC Source Current (I_{sl}) Controller by Type2 Fuzzy Logic Controller (FLC)

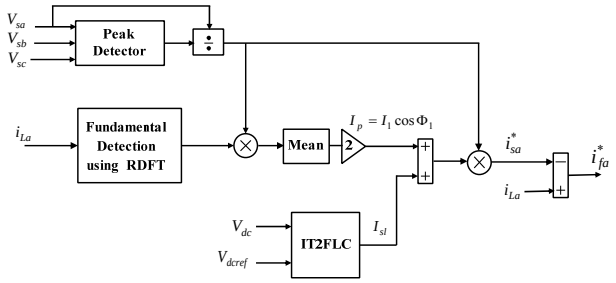

Fig. 3. Reference Current Extraction by the Proposed Method (Phase A)

The voltage of the DC side capacitor (V_{dc}) is identified and passed through the Butterworth design-based low pass filter with a cut-off frequency of 20 Hz to stabilize the measured DC link voltage and then compared with a reference value (V_{dcref}). The obtained errors are as follows:

(8) $$e(n) = V_{dcref}(n) - V_{dc}(n),\ \ ce(n) = e(n) - e(n-1)$$

where V_{dcref} is the reference DC side capacitor voltage, and *ce*(*n*) is the change in the error signal at the n^{th} sampling instant. The desired peak current of the AC source can be calculated as follows:

(9) $$I_{sp} = I_p + I_{sl}$$

As discussed above, the AC source currents must be sinusoidal and in phase with the source voltages. Therefore, the desired currents of the AC sources can be calculated by multiplying the peak source currents with the unit vectors of the three-phase source voltages. These unit vectors can be obtained using,

(10) $$u_{sa} = \frac{v_{sa}}{V_m}$$

The desired source side currents can be calculated from Equation (1) as follows:

(11) $$i_{sa}^{*} = I_{sp} u_{sa}$$

Finally, the reference currents of the APF can be obtained using the following equation:

(12) $$i_{fa}^{*} = i_{La} - i_{sa}^{*}$$

In this study, the fundamental current of the load current $i_L(t)$ is obtained using the RDFT block. The SAPF control block diagram is shown in Fig. 3.

Recursive Discrete Fourier Transform

Assuming that a signal $x(t)$ is sampled at a sampling frequency $f_s = 1/T_s = N/T_w$, where T_w is the time window for the DFT and N is the number of samples in the period T_W, a set of signal data $\{x_n\}$ with n data points is produced. The DFT of the m[th] harmonic at the time step k-1 at the frequency m/T_w is expressed as follows [16]:

(13) $$X_m(k-1) = \sum_{n=k-n}^{k-1} x_n \exp(-j2\pi(n-1)m/N)$$

At the time step k, a new sample of $x(t)$ exists, and the DFT for the new set of signal data is expressed as follows:

(14) $$X_m(k) = \sum_{n=k-n+1}^{k} x_n \exp(-j2\pi(n-1)m/N)$$

Subtracting Equation (14) from Equation (15), we get,

(15) $$X_m(k) - X_m(k-1) = [x_k - x_{k-1}]\exp(-j2\pi(k-1)m/N)$$

Thus, the signal data is expressed as follows:

(16) $$X_m(k) = X_m(k-1) + [x_k - x_{k-N}]\exp(-j2\pi(k-1)m/N)$$

A recursive method for the DFT of $\{x_n\}$ is expressed by Equation (16). A single harmonic component is provided by the inverse DFT from Equation (16). This inverse DFT at the frequency m/T_w for the m[th] harmonic is given by the following equation:

(17) $$x_m(k) = \Gamma(m) X_m(k) \exp(j2\pi(k-1)m/N)$$

The scaling factor Γ is defined as follows:

(18) $$\Gamma(m) = \begin{cases} N^{-1}, & m = 0, N/2 \\ 2N^{-1}, & \text{else} \end{cases}$$

Based on the above discussion, a block diagram for an RDFT filter (for m = 1) is shown in Fig. 4. In this study, the block diagram has an input (sampled in the load current $i_L(k)$) and output $i_1(k)$ (sampled in the fundamental component of the load current). T_W is equal to the system period (i.e., T_w = 0.02 s).

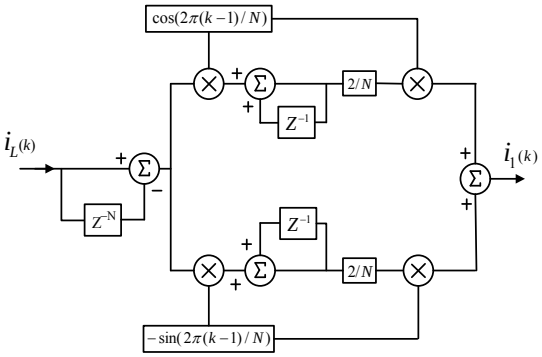

Fig. 4. RDFT Filter Block

Interval Type-2 Fuzzy Logic Based DC Bus Voltage Controller

When the model system is precisely known, FLCs are the superior choice [17]. The inputs of the FLC include the capacitor voltage deviation and its derivative, whereas the output of the FLC is the magnitude of the active current component corresponding to APF losses, as shown in Fig. 2.

For type-1FLC (T1FLC), the following fuzzy levels or sets are chosen to convert the input and output variables into linguistic variables: negative big (NB), negative medium (NM), negative small (NM), zero (ZE), positive small (PS), positive medium (PM), and positive big (PB) [18].

The T2FLC was first introduced by Zadeh in the 1970s as an extension of the type-1 fuzzy controller [19]. In this study, a type-1FLC is first modelled and then the same configuration is used to design the IT2 FLC configuration. Membership functions are selected for the input and output variables as presented in Figs. 5 and 6, respectively. In the steady state, small errors require fine control, which needs fine input/output variables. In the transient state, large errors require coarse control, which needs coarse input/output variables [20]. When all variables are determined, the rule-based elements of the table are ascertained. Both inputs have seven subsets according to the rule-based elements shown in Table 1 [18].

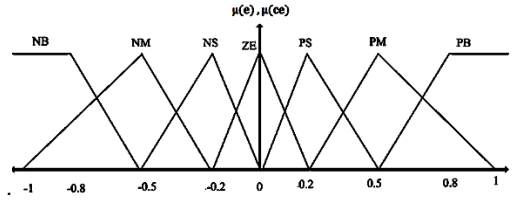

Fig. 5. Inputs of Normalized Membership Function

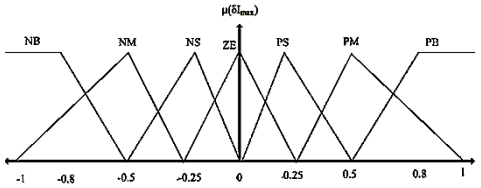

Fig. 6. Outputs of Normalized Membership Function

Table 1. Fuzzy Logic Control Rule

Input	Error (e)							
changing of error c(e)		NB	NM	NS	ZE	PS	PM	PB
	NB	NB	NB	NB	NB	NM	NS	ZE
	NM	NB	NB	NB	NM	NS	ZE	PS
	NP	NB	NB	NM	NS	ZE	PS	PM
	ZE	NB	NM	NS	ZE	PS	PM	PB
	PS	NM	NS	ZE	PS	PM	PB	PB
	PM	NS	ZE	PS	PM	PB	PB	PB
	PB	ZE	PS	PM	PB	PB	PB	PB

Similar to the conventional T1FLC, the T2FLC contains the following components: a fuzzifier, a rule base, a fuzzy inference engine, and an output processor that comprises a type reducer and a defuzzifier. The output processor of the T1FLC consists only a defuzzifier. Fig. 7 shows the structure of a T2FLC. The type reducer maps the T2FLC set into a type-1 fuzzy set and defuzzifier is implemented similarly with that of the T1FLC so that a fuzzy output is transformed into a crisp output.

In the type-2 fuzzy set, the membership grade for each element is also a fuzzy set in the range of 0 to 1 instead of a crisp number of either 0 or 1. The MFs of type-2 fuzzy sets are three-dimensional and include a footprint of uncertainty (FOU), as indicated by the shaded region bounded by the lower and upper MFs in Fig. 8. An FOU shows the uncertainties in the shape and position of the type-1 fuzzy set and provides an additional degree of freedom to control uncertainties.

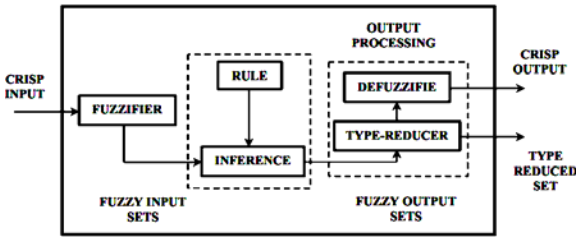

Fig. 7. Type-2 Fuzzy Logic Controller

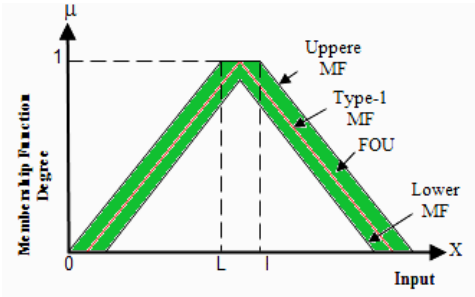

Fig. 8. Membership Function of Interval T2FLC

The outputs of the inference engine should be type-reduced and then defuzzified to create a crips output.The design of the IT2FLC for the DC voltage regulator is similarly configured as the conventional type-1FLC (Figs. 5 and 6). Two inputs (error and rate of error) and a single output in each set of the input /output variables have seven similar linguistic variables. The fuzzy labels are NB, NM, NS, ZE, PS, PM, and PB. The rules for IT2FLC are also similar to the T1FLC; however, their antecedents and consequents are represented by the IT2FLC. The diagonal rule table summarized in Table 1 is constructed for the scenario in which the error and the change of error approach zero with a fast rise time without overshoot. In this case, the Mamdani interval T2FLC is considered and the popular center-of-sets approach is assigned for the type-reduction method. The Karnik–Mendel algorithm is then used to obtain the type-reduced set.

The IT2FLC was implemented in source codes using MATLAB software in m-codes. The source codes were embedded in the MATLAB Function Block for incorporation into the Simulink model. The capacitor voltage deviation $e(n)$ and its derivative $ce(n)$ are fed into the developed function block as the input and the output of the AC source current (I_{sl}).

Adaptive Interval Type-2 Fuzzy HB Current Control

The fixed-hysteresis current controller has unpredictable switching functions; the method affects the efficiency and reliability of the AFP. The defects of the fixed-hysteresis current controller can be resolved using the adaptive-hysteresis current controller. However, the adaptive hysteresis current controller causes more switching power losses because of high switching frequency. This obstacle is solved by the proposed fuzzy method for adaptive hysteresis current controller. The hysteresis bandwidth is computed using FLC to reduce switching power losses.

To control the switching pattern of the inverter, a HB can be modulated at different fundamental frequency cycle points. The hysteresis band is given (for phase a) by [20]:

$$HB = \left\{ \frac{0.125 V_{dc}}{L f_c} \left[1 - \frac{4L^2}{V_{dc}^2} \left(\frac{v_s}{L} + m \right)^2 \right] \right\} \quad (19)$$

Where: f_c - frequency of modulation, $m = \frac{di_{fa}^*}{dt}$: the slope of command current wave, L : coupling inductance, and V_{dc} : the DC link capacitor voltage.

As shown in Equation (19), the HB is a function of supply voltage, DC link voltage, and reference current variations of modulation (m) which can be controlled to minimize the effects of current distortion on modulated waveforms. The three-phase HB profiles, namely, HBa, HBb, and HBc, should be the same for different phases to obtain symmetrical operations of the three phases.

The modulation frequency remains almost constant, and the performances of PWM and SAPF are substantially improved. Fig. 9 shows the block diagram of the adaptive HB computation for phase A.

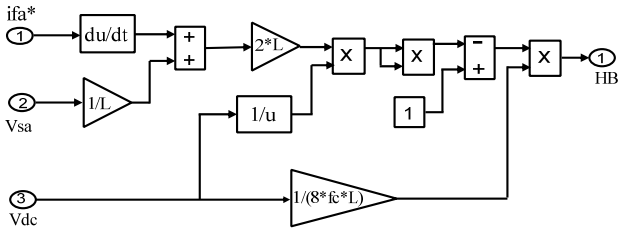

Fig. 9. Block Diagram of the Adaptive Hysteresis Bandwidth Computation

Also, Fig. 10 presents a block diagram of the adaptive IT2FL HB current control. In this case, the supply voltage, $v_s(t)$ and the APF current reference slope di_f^*/dt and the HB magnitude can be selected as the input and output variables of the fuzzy controller, respectively, as expressed in Equation (19). Based on T1FLC, which is described below, IT2FL is designed to produce proper HBs. A triangular MF is selected for its simplicity and ease of implementation. Fig. 11 shows the MFs used for fuzzification in this application according to [21].

Regarding the discourse universe of the MFs (-1, 1), (-0.5, 0.5), and (0, 1), as described in Fig. 11, the three numbers are set (b1, c1, and b2); the numbers deputize the values of the discourse universe corresponding to the minimum of left, peak, and minimum of right of the triangle of the MF, respectively. Therefore, five primary fuzzy sets labelled as {normal large (NL), normal medium (NM), zero error (ZE), positive medium (PM), and positive large (PL)} are used as inputs to construct a rule base. Moreover, five fuzzy sets labelled as {positive very small (PVS), PS, PM, PL and positive very large (PVL)} are used as the output variable of the HB. The antecedent (IF) – consequence (THEN) form is used to express the fuzzy rule. The fuzzy rule according to [22] is presented in Table 2. Based on the developed T1FLC and the above discussion, IT2FLC for HB current control is designed with two input selections: ($v_s(t)$ and di_f^*/dt). The FLC produces the desired output (HB magnitude).

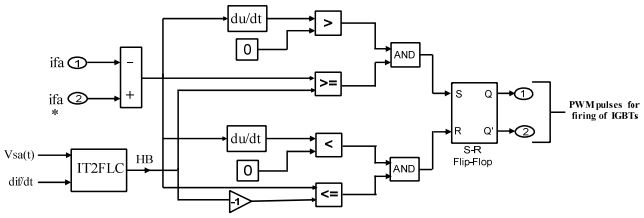

Fig. 10. Interval Type2 Fuzzy HB Current Control

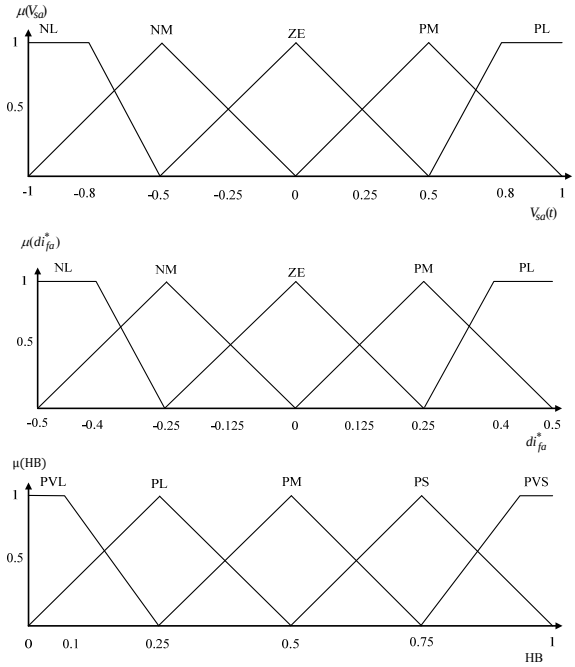

Fig. 11. Membership Functions for Input Variables $V_s(t)$, di_f^*/dt and Output Variable HB

Table 2. Fuzzy Control Rule

		$V_s(t)$				
		NL	NM	ZE	PM	PL
di_f^*/dt	NL	PVS	PS	PS	PM	PM
	NM	PS	PS	PS	PM	PM
	ZE	PL	PL	PVL	PL	PL
	PM	PM	PM	PS	PS	PS
	PL	PM	PM	PS	PS	PVS

Test System Description

Simulations were conducted on the test system referring to Fig. 1 to compare the performance of the SAPF using two different current controllers: adaptive HB current controller and adaptive interval type2 fuzzy HB current controller. The test system consists of a three-phase voltage source, a SAPF, and an uncontrolled rectifier with R and L loads that generate harmonic currents in the supply system. The filter inductor, namely, inductor L_f and resistor R_f are also used to connect the SAPF to the test system.

The main SAPF component is a VSI that includes a DC link. On the DC side of the inverter, a DC-link capacitor C_{dc} is coupled. The VSI consists of self-commutating IGBT switches parallel to the PCC) that is connected to the filter inductors (R_f, L_f). The filter inductors eliminate the harmonics caused by the switching of the IGBT inverter, provide isolation, and smoothen high-frequency components. To suppress switching spikes, a smoothing inductor (R_{sm}, L_{sm}) in every phase is connected in series with the nonlinear load. The system parameters are given in Table 3.

Table 3. Circuit Parameters of the SAPF

Parameter	Numerical Value
Source Voltage	312 V (peak) , 50 Hz
Source Resistance and Inductance	0.1 ohm , 1 mH
Filter Inductance, Resistance	1 mH , 0.1 ohm
Load Resistance and Inductance	10 Ω , 5 mH
DC Capacitor	2500 μF
DC Capacitor Reference Voltage	650 V
Sample Time (Ts)	10 μs

Simulation Results

The values of total harmonic distortion, power factor, and reactive power measured at the PCC are shown in Table 4. Fig. 12 illustrates the source currents without SAPF. The source currents after compensation are shown in Figs. 13 and 14. The results of Figs. 12, 13, and 14 show that the source currents only consist of fundamental currents.

Table 4. Total Harmonic Distortion, Power Factor, and Reactive Power

Method used	**Source Current (phase a)THD%**	**Power Factor**	**Reactive Power(Var)**
Before shunt compensation	21.03	0.9541	2616
With adaptive interval type2 fuzzy HB current controller	2.12	1	6.284
With adaptive HB current controller	2.57	1	30.76

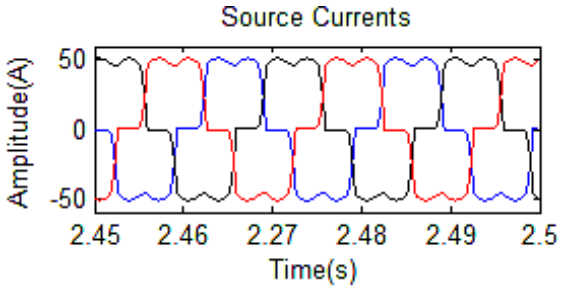

Fig. 12. Source Currents without SAPF

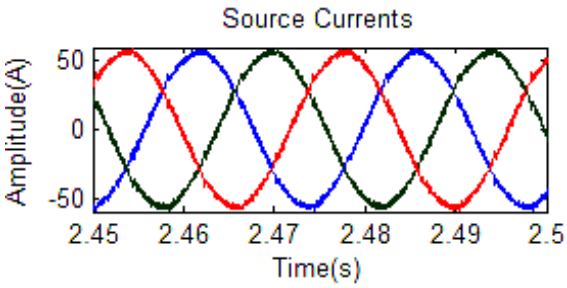

Fig. 13. Source Currents for SAPF with the conventional adaptive HB current controller

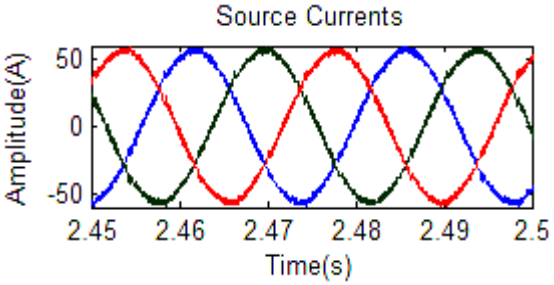

Fig. 14. Source Currents for SAPF with adaptive interval type2 fuzzy HB current controller

From Table 4, the network with SAPF is concluded to have much less harmonics than a network without SAPF. The total harmonic distortion (THD) of the supply current is reduced to approximately 2% from 21.03%. The THD is well below the required standard (5%). Reactive currents are considerably restrained after compensation (from 2616 Var to 30.76 Var). The comparison of results in Table 4 indicate that the proposed current controller achieves better results compared with the conventional adaptive HB current controller in reducing harmonics and improving power factors by the SAPF.

Conclusion

This paper presented a novel current controller with a type2 fuzzy HB and a novel control technique based on RDFT to calculate the reference current for the APFs of three-phase systems. The SAPF was simulated and its performance was analyzed in a sample power system. The results of the simulation on the test system show that THDs are significantly reduced and the power factor is improved using the proposed current controller. Compared with the conventional adaptive HB current controller, the proposed controller is more effective in reducing THD and reactive power in which the THD of source current is 2.12% versus 2.57%, and for reactive power 6.284 Var versus 30.76 Var.

REFERENCES

[1] Francisco De la Rosa, Harmonics and Power System , Taylor & Francis Group, 2006.

[2] A. Bhattacharya, C. Chakraborty,"A shunt active power filter with enhanced performance using ANN-based predictive and adaptive controllers," IEEE Trans. Ind. Electron., vol. 58, no. 2, pp. 421–428,Feb. 2011.

[3] S. Rahmani, N. Mendalek, and K. Al-Haddad,"Experimental design of a nonlinear control technique for three-phase shunt active power filter,"IEEE Trans. Ind. Electron., vol. 57, no. 10, pp. 3364–3375, Oct. 2010.

[4] K. Al-Haddad, B. Singh, B. N. Singh and A. Chandra, "An Improved Control Algorithm of Shunt Active Filter Voltage Regulation, Harmonic Elimination, Power-Factor Correction, and Balancing of Non-Linear Loads," IEEE Transaction on Power Electronics 15 No. 3, 495–507, 2004.

[5] L. H. Tey, P. L. So and Y. C. Chu, "Improvement of power quality using adaptive shunt filter," IEEE Trans. Power Del., vol. 20, no. 2,pp. 1558-1568, April 2005.

[6] S.H. Fathi, M. Pishvaei, and G.B. Gharehpetian,"A frequency domain method for instantaneous determination of reference current in shunt active filter," TENCON, IEEE Region 10 Conference,1-4, 2006.

[7] Z. Salam, P. C. Tan, and A. Jusoh,"Harmonics mitigation using active power filter: A technological review," Elektrika Journal of Electrical Engineering, 8: 17-26, 2006.

[8] T. Komrska, J. Žák, and Z. Peroutka,"Control strategy of active power filter with adaptive FIR filter-based and DFT-based reference estimation," Power Electronics Electrical Drives Automation and Motion (SPEEDAM), 2010 International Symposium on, Page(s): 1524 – 1529, 2010.

[9] G. Chen, Y. Jiang, and H. Zhou, "Practical Issues of Recursive DFT in Active Power Filter Based on CPC Power Theory, "Power and Energy Engineering Conference, APPEEC 2009. Asia-Pacific, 1 – 5, 2009.

[10] H. Akagi, Yoshihira Kanazawa, and Akira Nabae,"Instantaneous Reactive Power Compensators Comprising Switching Devices Without Energy Storage Components, " IEEE Transactions On Industry Applications, Vol. IA20, No.3, May/June1998.

[11] M.A Kabir, U. Mahbub," Synchronous Detection and Digital control of Shunt Active Power Filter in Power Quality Improvement," IEEE Power and Energy Conference at Illinois (IEEE PECI), University of Illinois at Urbana-Champaign, USA, 2011.

[12] A. Khoshkbar Sadigh, M. Farasat, S.M. Barakati,"Active power filter with new compensation principle based on synchronous reference frame," North America Power Symposium (NAPS),DOI: 10.1109/NAPS.2009.5484077,2009.

[13] F.Mekri, B. Mazari and M. Machmoum ,"Control and optimization of shunt active power filter parameters by fuzzy logic," Canadian Journal of Electrical and Computer Engineering, vol.31, no.3, pp.127-134, 2006.

[14] H.Hagras, "Type-2 FLCs: A new generation of fuzzy controllers," IEEE Computational Intelligence Magazine, 2: 30-43, 2007.

[15] P. Karuppanan , K.K. Mahapatra,"Fuzzy Logic Controlled Active Power Line Conditioners for Power quality Improvements," International Conference on Advances in Energy Conversion Technologies (ICAECT 2010), Jan07 -10, 2010.

[16] E. O. Brigham, the Fast Fourier Transform. Englewood Cliffs, NJ: Prentice-Hall, 1974.

[17] P . Karuppanan , K. K. Mahapatra , "PI and fuzzy logic controllers for shunt active power filter — A report," ISA Transactions vol. 51 issue 1 January, p. 163-169, 2012.

[18] P . Karuppanan , K. K. Mahapatra , "PLL with PI, PID and Fuzzy Logic Controllers based Shunt Active Power Line Conditioners," IEEE International Conference on Power Electronics, Drives and Energy Systems-Dec 21 o 23, 2010.

[19] L. A. Zadeh, "The concept of a linguistic variable and its application to approximate reasoning-1," Inf. Sci., vol. 8, pp. 199-249, 1975.

[20] M. Suresh, A. K. Panda and Y. Suresh, "Fuzzy Controller Based 3Phase 4Wire Shunt Active Filter for Mitigation of Current Harmonics with Combined p-q and Id-Iq Control Strategies," Journal of Energy and Power Engineering, Vol. 3, No.1, pp. 43-52, 2011.

[21] P. Rathika , D. Devaraj, " Fuzzy Logic – Based Approach for Adaptive Hysteresis Band and Dc Voltage Control in Shunt Active Filter, " International Journal of Computer and Electrical Engineering vol. 2, no. 3, pp. 404-412, 2010.

[22] M.B.B. Sharifian, R. Rahnavard and Y.Ebrahimi, "Variable Hysteresis Band Current Controller of Shunt Active Filter Based Fuzzy logic Theory under Constant Switching Frequency", International Journal of Computer and Electrical Engineering, International Association of Computer Science and Information Technology Press (IACSIT), Singapour, ISSN Print: 1793-8163, ISSN Online 1793-8198, Vol. 1, No. 2, pp. 1793-8198, June 2009.

Authors: *Hamid Reza Imani Jajarmi, Prof. Dr. Azah Mohamed, Dr. Hussein Shareef and Dr. Subiyanto are with the Department of Electrical, Electronic and Systems Engineering, University Kebangsaan Malaysia (UKM), 43600 Bangi, Selangor, Malaysia, E-mail: imani145@gmail.com; azah@eng.ukm.my; shareef@eng.ukm.my; biyantote_unnes@yahoo.com*